INTERNATIONAL JOURNAL OF HYDROGEN ENERGY XXX (2014) 1–8

Available online at www.sciencedirect.com

ScienceDirect

journal homepage: www.elsevier.com/locate/he

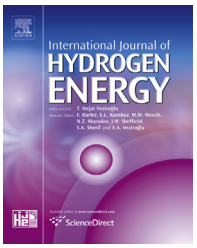

Influence of activated carbon porous texture on catalyst activity for ethanol electro-oxidation

Elen Leal da Silva [a,*], *Maria Rita Ortega Vega* [a], *Patrícia dos Santos Correa* [a], *Andrés Cuña* [b], *Néstor Tancredi* [b], *Célia de Fraga Malfatti* [a]

[a] *LAPEC/PPGE3M, Universidade Federal do Rio Grande do Sul, Brazil, Av. Bento Gonçalves, 9500, Setor 4, Prédio 75, Sala 232, 91501-970, Porto Alegre, RS, Brazil*

[b] *Universidad de la República (UDELAR), Facultad de Química, Avenida General Flores 2124, CC 1157, 11800, Montevideo, Uruguay*

ARTICLE INFO

Article history:
Received 1 April 2014
Received in revised form
10 July 2014
Accepted 19 July 2014
Available online xxx

Keywords:
Biocarbon
Eucalyptus grandis
Cyclic voltammetry
Platinum-based catalyst

ABSTRACT

Direct ethanol fuel cells are based in ethanol electro-oxidation at low temperature and they constitute an alternative energy conversion system. However, they need catalysts in order to improve their efficiency, given that ethanol electro-oxidation is a slow-kinetic reaction. Among those catalysts platinum and platinum alloys play an important role in the increase of the ethanol cleavage kinetics for fuel cell application. However, to maximize the catalyst performance, support materials are needed in order to reduce the catalyst load considering its high cost. One of the more versatile catalyst supports is activated carbon. Recently, attention has focused on wood as carbon material precursor, because of its sustainability and also because the obtained carbons have excellent final properties. In the present work, activated carbon obtained by physical activation of *Eucalyptus grandis* wood (biocarbon) was tested as Pt and PtSn catalyst support, for ethanol electro-oxidation reaction. For comparison purposes, commercial activated carbon Vulcan XC72 was also tested. The catalyst supports were characterized by textural analysis, elemental analysis and infrared spectroscopy. The obtained catalysts were characterized regarding structure by XRD and their electrochemical behavior was evaluated by cyclic voltammetry. Biocarbon-supported PtSn electrocatalysts showed better electrochemical performance related to the commercial activated carbon (Vulcan XC72)-supported ones, since its developed current density and potential were the highest and its onset potential was the lowest. However, pure platinum showed better values for current density, potential and onset potential in Vulcan XC72-based activated carbons, being the untreated one the best support in this case.

* *Corresponding author*. Av. Bento Gonçalves, 9500, DEMET, Prédio 75, Sala 232, CEP 91501-970, Porto Alegre, RS, Brazil. Tel.: +55 51 33089406.

E-mail addresses: elenlealdasilva@gmail.com, elen.leal@ufrgs.com, elen.leal@hotmail.com (E.L. da Silva), mortegavega811@gmail.com (M.R. Ortega Vega), patricia.correa@ufrgs.br (P.S. Correa), acuna@fq.edu.uy (A. Cuña), nestor@fq.edu.uy (N. Tancredi), celia.malfatti@ufrgs.br (C.F. Malfatti).

http://dx.doi.org/10.1016/j.ijhydene.2014.07.103

Introduction

Energy conversion from renewable sources has motivated the development of new technologies, aiming to increase the transformation efficiency. In this context, Direct Ethanol Fuel Cells (DEFC) have been seen as environmentally viable alternative energy sources [1].

DEFC are low temperature fuel cells, whose redox reactions have slow kinetics. It makes necessary the use of noble electrocatalysts, capable of accelerating those reactions. Platinum is well known as the most suitable catalyst for fuel cell reactions because of its excellent catalytic activity and stability, mainly in acidic media [2].

Regarding platinum-based electrocatalyst, it is also well known that the natural reservoirs and the price of this metal are the main factors because of which alternatives are sought. Among those alternatives, there is the incorporation of the minimum necessary Pt amount, as well as the setting of the adequate conditions to enhance its activity. In this case, heterogeneous catalysis can be applied in order to use a catalyst deposit (support) with the higher surface area and with extremely small catalysts particles (nanoparticles) [3]. These particles may be composed of pure platinum or an alloy constituted by platinum and another metal. These metals or alloys are dispersed in a conductive carbonaceous matrix that works as catalyst support [4].

Namely, platinum is the best catalyst for ethanol electro-oxidation reaction. However, its catalytic surface can be quickly poisoned due to the strong adsorption of intermediate species, mainly carbon monoxide, which results of uncompleted ethanol oxidation [4]. The purpose of another element onto the platinum, as a co-catalyst, not only aims to a catalytic activity increase, but to poisoning prevention and the way to guarantee the fuel cell performance.

Supported metal and metal oxide catalysts are indispensable for energy and chemical industries to reduce consumption of raw materials and to minimize the production of waste. Control over the preparation of supported metal catalysts is necessary to improve their key properties as activity, selectivity, and stability [5].

Support materials have an enormous influence on the catalyst performance, taking into account that the support settles the particle distribution, electrochemically active area, catalyst stability, mass transport and electronic conductivity. Also, catalyst needs a high surface area that can be enhanced by the support. An optimal catalyst support can diminish the required catalyst amount and thus its cost. Recent studies revealed that the carbonaceous support properties can affect significantly the electrochemical properties of the catalyst in a fuel cell [6]. It was stated that carbon materials with high surface area not only may increase the platinum nanoparticles dispersion but ease the electron transfer, which improves the fuel cell performance.

The advent of nanostructured support materials such as ordered mesoporous materials, carbon nanofibers, and carbon nanotubes provides opportunities for novel supported metal and metal oxide catalysts. Carbon nanofibers and carbon nanotubes are promising support materials in view of, among others, the control of surface properties, chemical inertness, the high accessibility, thermal stability, mechanical strength, and tunable bulk density [5,7,8]. These properties are also present in activated carbon.

Activated carbon precursor can be vegetal or mineral. Mineral carbon is a natural fossil fuel extracted from the Earth through mining, while, vegetal activated carbon is obtained from biomass, through a carbonization process.

Commercial Vulcan XC72 (Cabot Co.) is obtained by thermal hydrocarbon decomposition and it is constituted basically by carbon spherical nanoparticles with colloidal size, that get together to form aggregates or agglomerates [9]. This carbon has been widely used as catalyst support.

Among the materials used for obtaining activated carbon, wood and coconut shell can be mentioned [10]. Due to its high availability and low sulfur percentage, wood as activated carbon precursor is economically viable and environmentally interesting.

Eucalyptus is a worldly cultivated tree, whose growth is very fast. Its wood is used for furniture and to obtain cellulose pulp. Since some years ago, it has been used to develop highly microporous activated carbon [11–13]. Also, this precursor is renewable and has low cost. On the other hand, there is no background about the application of this kind of activated carbons as platinum- or platinum alloy-based catalyst supports.

In this work, activated carbons obtained by physical activation of *Eucalyptus grandis* wood and a commercial Vulcan XC72R were tested as Pt and PtSn catalyst support, for ethanol electro-oxidation reaction.

Experimental

Carbonaceous catalyst support synthesis

Three different catalyst supports for the Pt and PtSn catalysts were tested in this work. Their descriptions can be found in Table 1:

Table 1 – Carbons and activated carbons used as catalyst supports.

Samples	Description
Vulcan	Carbon Vulcan XC72R, supplied by Cabot Co., used without treatment.
a-Vulcan	Carbon Vulcan XC72R, activated in CO_2 atmosphere, at 800 °C for 2 h.
a-BC	Biocarbon obtained from *Eucaliptus grandis* wood activated in CO_2 atmosphere, at 800 °C for 2 h.

Please cite this article in press as: da Silva EL, et al., Influence of activated carbon porous texture on catalyst activity for ethanol electro-oxidation, International Journal of Hydrogen Energy (2014), http://dx.doi.org/10.1016/j.ijhydene.2014.07.103

Catalysts synthesis

Electrocatalysts synthesis was already explained in a former work [14]. Impregnation/reduction method was employed, using ethylene glycol as reduction agent and $H_2PtCl_6.6H_2O$, $SnCl_2.2H_2O$ salts as catalyst precursors. Carbons were impregnated with the particles with a metallic load of 40% wt. The composition of the catalysts and the used supports are shown in Table 2.

Support characterization

Textural analysis

The supports porous texture was determined by adsorption/desorption of N_2 at 77 K isotherm, with Beckman Coulter SA 3100 equipment. Isotherm analysis was done by Brunauer–Emmet–Teller (BET) equation. Total pore volume at relative pressure of 0.99 and specific surface (S_{BET}) were determined. Mean pore size (L) was calculated by:

$$L(\text{nm}) = \frac{4000 V_T\left(\frac{\text{cm}^3}{\text{g}}\right)}{S_{BET}\left(\frac{\text{m}^2}{\text{g}}\right)} \quad (1)$$

The micropore surface area (S_{mic}) was determined by the Dubinin–Radushkevich method.

Ash content

Ash content was determined according to ASTM D2866/2011 [15], and computed by:

$$\%\text{Total Ash} = \frac{C - A}{B - A} \times 100 \quad (2)$$

Where A is the crucible weight in grams (g), B is the crucible weight plus the original sample (g) and C is the crucible weight with the incinerated sample (g).

Volatile matter corresponds to the weight loss.

Elemental analysis

Elemental composition (nitrogen, hydrogen, carbon and sulfur) was determined with a Termo Scientific Flash 2000 equipment. The oxygen content was determined by difference.

Table 2 – Systems of catalysts and catalyst supports.

Samples	Description
Pt/Vulcan	Untreated Vulcan XC72 supported Pt
Pt/a-Vulcan	a-Vulcan supported Pt
Pt/a-BC	a-BC Biocarbon supported Pt
PtSn/Vulcan	Untreated Vulcan XC72 supported Pt:Sn 79:21 alloy
PtSn/a-Vulcan	a-Vulcan supported Pt:Sn 79:21 alloy
PtSn/a-BC	a-BC Biocarbon supported Pt:Sn 79:21 alloy

Infrared spectroscopy

All the samples were analyzed by Fourier transform infrared spectroscopy, using a Shimadzu IRPrestige-2 equipment, to identify the chemical functions present on the activated carbon surface. For the analysis, carbon was diluted in a KBr pellet.

Catalysts characterization

X-Ray diffraction

X-Ray diffraction analysis was made with a Philips, X'Pert MPD equipment, operating with Cu-Kα radiation, generated with 40 kV and 40 mA. X-Ray diffractogram allows establishing the crystal structure assumed by the catalyst inside the support.

Cyclic voltammetry

Cyclic voltammetry was done in order to determine the electrochemical behavior of the catalyst in 1.0 M ethanol – 0.5 M H_2SO_4 solution. Measurements were carried out at 25 °C, in deaereated medium, bubbling nitrogen inside the solution since 10 min before, in order to eliminate the oxygen present in the medium. At least, three repetitions of the measurements were done, using a potentiostat/galvanostat Omnimetra PG39A, with scan rate of 20 mV/s [16], in a potential range from −0.04–0.96 V versus saturated calomel electrode (SCE). The voltammograms presented in this work represent the tenth voltammetric cycle applied upon each material. A three-electrode cell was used, with platinum as counter-electrode and SCE as reference electrode. As working electrode a graphite disk was used with a geometric area of 0.29 cm^2, which was coated with a mixture of catalyst powder in Nafion®. The preparation procedure of the working electrodes consisted of dispersing supported catalysts particles in ethanol (Merck) and Nafion® (5% wt, Aldrich). After that, the electrodes were dried in an oven at 25 °C, aiming to evaporate the ethanol.

Results and discussion

Textural analysis

Table 3 shows the textural characterization results for the catalyst supports.

A significant difference in surface area between commercial carbons and biocarbon is observed. Biocarbon had a surface area very much higher than the one for the Vulcan precursor carbons; also its microporous surface was considerably higher than the ones for Vulcan and a-Vulcan.

Table 3 – Textural characterization for the activated carbons.

Sample	V_T (cm^3/g)	S_{mic} (m^2/g)	S_{BET} (m^2/g)	L (nm)
Vulcan	0.44	103	216	8.20
a-Vulcan	0.39	86	230	6.88
a-BC	0.47	632	787	2.41

Please cite this article in press as: da Silva EL, et al., Influence of activated carbon porous texture on catalyst activity for ethanol electro-oxidation, International Journal of Hydrogen Energy (2014), http://dx.doi.org/10.1016/j.ijhydene.2014.07.103

Table 4 – Elemental analysis results for the catalyst supports and for the precursor *Eucalyptus grandis*.

Sample	C%	H%	N%	S%	Ash%	O%
Vulcan	96.42	0.61	0.00	0.61	2.16	0.20
a-Vulcan	96.39	0.50	0.00	0.44	2.38	0.29
Eucaliptus grandis Wood	49.50	6.50	0.00	0.00	0.40	43.6
a-BC	82.16	1.75	0.00	0.00	6.10	9.86

Although a sample of Vulcan was submitted to activation (a-Vulcan), the surface area showed a slight increase meanwhile the pore size and volume slightly diminished. These changes can be due to a micropore widening that took place during the activation process and force this trend. Henceforth, it can be stated that Vulcan carbon did not suffered significant alterations in its porous texture with the activation. The predominant texture for all the activated carbons was mainly mesoporous (2 nm < L_{pore} < 50 nm).

Elemental analysis

Table 4 shows the C, H, N, S, O and ash percent for the studied carbons and for the biocarbon precursor, *E. grandis*.

Vulcan carbon showed high carbon content and low oxygen percentage (less than 1%). It can be seen that sulfur content is not negligible for the mineral support, being higher than oxygen content, which is explained by its obtaining way. Biocarbon does not show sulfur content because there is not sulfur in the precursor.

a-Vulcan carbon has a similar composition to Vulcan. This result is expected, taking into account that physical activation with CO_2 atmosphere induces the development of porosity and eliminates hydrogen and oxygen from the carbonaceous matrix, confirming the Vulcan low reactivity with CO_2 [17,18].

Infrared spectroscopy

Fig. 1 shows the infrared spectra for the studied supports.

According to Fig. 1 and Table 5, all the samples showed strong C=O stretching between 1750 cm^{-1} – 1250 cm^{-1} that correspond to carboxylic (1700 cm^{-1}) and lactonic (1730–1705 cm^{-1}) groups. Also, there is the presence of an –OH in-plane bending (1430 cm^{-1}). These oxygenated groups match with the oxygen content in the elemental analysis.

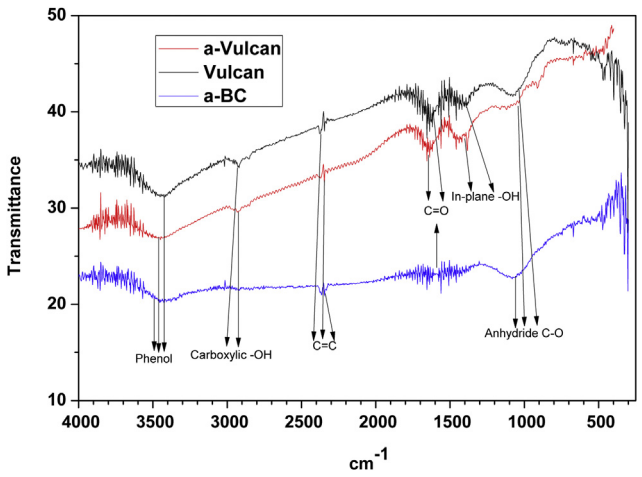

Fig. 1 – Infrared spectra for Vulcan, a-Vulcan and a-BC carbons.

Table 5 – Lattice parameters and crystallite sizes for the studied electrocatalysts.

Sample	Lattice parameter (Å)	Crystallite size (nm)
Pt/Vulcan	3.92	4.72
Pt/a-Vulcan	3.92	3.00
Pt/a-BC	3.91	4.81
PtSn/Vulcan	3.96	3.03
PtSn/a-Vulcan	3.94	3.00
PtSn/a-BC	3.95	3.15

After the Vulcan activation, it is noticeable that the chemical functions are maintained in the a-Vulcan, because the presence of the former bands does not change. Furthermore, Vulcan carbons show structures with C=C bonds (2260 cm^{-1}), an anhydrous C–O stretching (1300 cm^{-1}) and an –OH carboxylic stretching at 2900 cm^{-1}. Also there is a phenolic stretching (3500 cm^{-1}) that appears to be stronger in the untreated Vulcan. 700–400 cm^{-1} band corresponds to –OH (hydroxyl groups) stretching. Untreated Vulcan shows lower oxygen content and a higher hydrogen percentage as seen in the elemental analysis, which matches with the presence of a hydroxyl band (1200–1000 cm^{-1} and 700–400 cm^{-1}). That hydroxyl band disappeared for a-Vulcan; it can be explained by the bonding of the oxygen inside the molecules instead of being a functional group, as well as the elimination of these atoms during the activation [16,17,19].

Biocarbon a-BC shows a C=C aliphatic stretching (2260 cm-1), as well as a phenolic stretching between 3550 and 3500 cm^{-1} and a lactonic band between 1700 and 1500 cm^{-1}. There are also strong in-plane and out-of-plane bendings (1275–1000 cm^{-1} and 700 cm^{-1} respectively), typical for C–H bonds in aromatic structures.

Catalyst characterization

X-Ray diffraction

X-Ray diffractograms for the supported metallic catalysts are shown in Fig. 2.

2θ angles for the maximum diffraction peaks were determined from the X-Ray diffraction. Zhou et al. [20] attributed the diffraction peaks at 39°, 46°, 68° e 81° to the (1 1 1) (2 0 0) (2 2 0) e (3 1 1) planes for platinum; they show a typical centered face cubic (CFC) crystal structure for crystalline platinum. Peak at 87° corresponds to (2 2 2) plane, that also belongs to CFC platinum [21]. Peaks found for the catalysts show angles similar to those related, revealing a CFC crystal structure for platinum.

Comparing synthesized electrocatalysts it is possible to observe that PtSn alloys have average lattice parameter value higher, in comparison with pure platinum. It involves a crystal grid dilatation.

Equation (3), based on the Bragg's law [22] is valid for crystalline cubic symmetry [23] and it can be used to estimate lattice parameter *a*.

Please cite this article in press as: da Silva EL, et al., Influence of activated carbon porous texture on catalyst activity for ethanol electro-oxidation, International Journal of Hydrogen Energy (2014), http://dx.doi.org/10.1016/j.ijhydene.2014.07.103

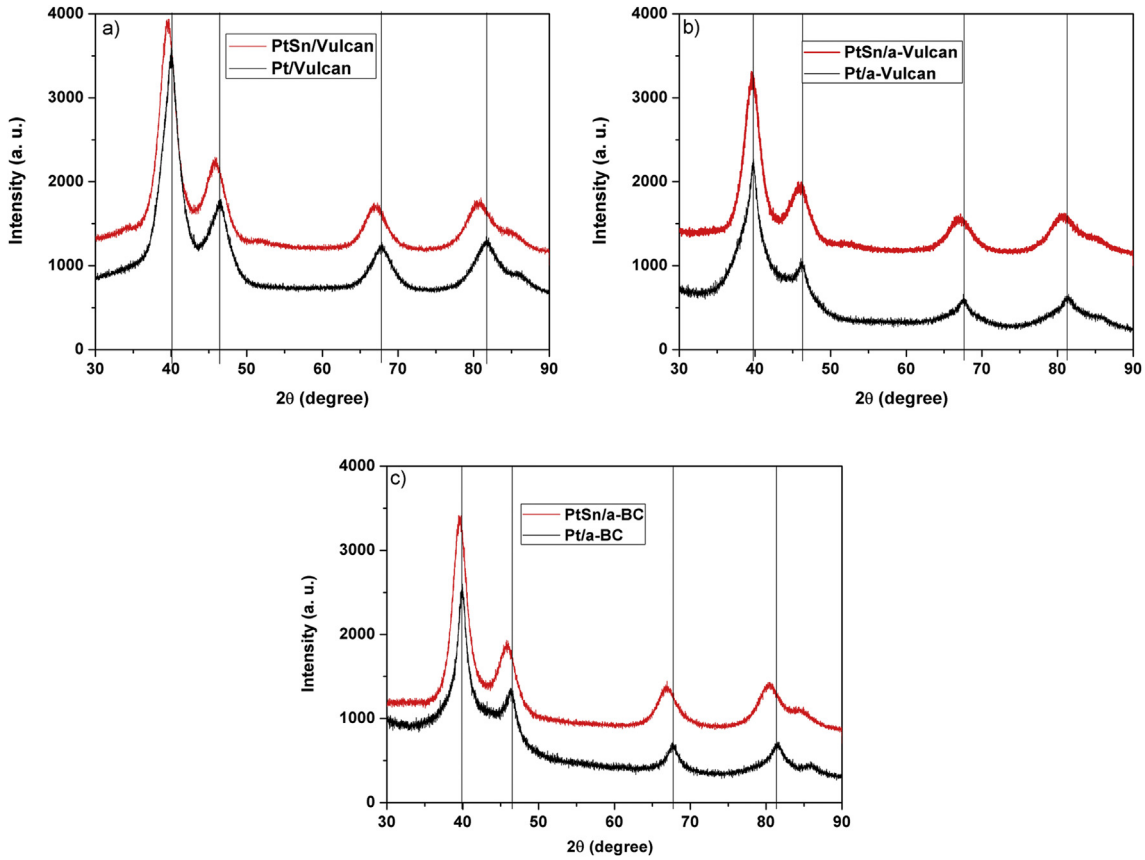

Fig. 2 – X-Ray diffractogram for a) Vulcan, b) a-Vulcan and c) a-BC supported Pt and PtSn catalysts.

$$a = \frac{n\lambda}{2sin\theta}.\sqrt{h^2 + k^2 + l^2} \quad (3)$$

Where, n represents the reflection order (it was considered $n = 1$ – first order reflection), λ is the wavelength (1.5418 nm for Cu-Kα radiation), θ is the half of 2θ of the four peaks and h, k, l are the Miller index for (1 1 1) (2 0 0) (2 2 0) and (3 1 1) planes. For each planes, it was determined a lattice parameter value, and an average value is presented in Table 6.

Comparing the systems Pt/Vulcan, Pt/a-Vulcan, Pt/a-BC, PtSn/Vulcan, PtSn/a-Vulcan and PtSn/a-BC, it is observed that Sn addition brings about the peak shift for lower 2θ angle values, compared with pure platinum. Similar results were already reported by other author [14,24], and the peak shift in the PtSn spectrum was attributed to the formation of a PtSn alloy and not only the deposition of these elements separately. Dilatation of crystal lattice can facilitate the C–C bond cleavage, which enhances the catalyst activity related to pure platinum and, hence, it contributes for the ethanol oxidation. Also, when tin forms alloy with platinum, it can transfer its electronic charge due to the low tin electronegativity and weaken the Pt–C ligand bond. In consequence, there is a reduction in poisoning caused by adsorbed reaction intermediates [14].

Crystallite size was also estimated from diffractograms by Scherrer's Equation (4) [25].

$$\tau = \frac{(k.\lambda)}{(\beta.\cos\theta)} \quad (4)$$

Where τ is the crystallite size (in nanometers), λ is the wavelength (in nanometers), β is the full width at half-maximum (FWHM) (in radians) of the diffraction peak (2 2 0), k is a

Table 6 – Maximum current density and potential for oxidation in the direct and reverse voltammetric scans.

Sample	Direct scan			Reverse scan	
	i (mA.cm^{-2})	E_{max} (mV)	E_{onset} (mV)	i (mA cm^{-2})	E_{max} (mV)
Pt/Vulcan	24.98 ± 11.83	824.33 ± 27.59	287.67 ± 32.33	31.34 ± 14.97	656.00 ± 72.79
Pt/a-Vulcan	29.91 ± 10.76	804.00 ± 63.15	157.00 ± 10.00	28.58 ± 9.41	576.33 ± 81.68
Pt/a-BC	19.16 ± 0.81	770.66 ± 20.50	291.33 ± 36.75	10.00 ± 0.42	470.33 ± 19.73
PtSn/Vulcan	52.00 ± 5.87	824.61 ± 17.17	134.60 ± 5.00	55.25 ± 6	705.00 ± 23.35
PtSn/a-Vulcan	52.00 ± 10.25	818.66 ± 10.96	187.33 ± 22.12	49.67 ± 18	656.66 ± 64
PtSn/a-BC	64.94 ± 1.70	902.00 ± 13.52	87.20 ± 43.00	53.67 ± 4.02	751.00 ± 24.98

Please cite this article in press as: da Silva EL, et al., Influence of activated carbon porous texture on catalyst activity for ethanol electro-oxidation, International Journal of Hydrogen Energy (2014), http://dx.doi.org/10.1016/j.ijhydene.2014.07.103

constant (0.94 to spherical crystallites) and θ is the diffraction angle. The crystallite size values are shown in Table 5.

From Table 5, PtSn alloys showed smaller crystallite size, independent of the support. For the activated Vulcan, crystallite size did not change for both Pt and PtSn alloy. May be, it can be related to a higher dispersion of the alloy in the support; i.e. there is less nucleation of the nanoparticles inside the support, which creates a higher number of active sites. In addition, it can be seen that the adsorption of the metal species crystallites, Pt and Pt–Sn alloy, takes place on the mesopores, regarding that the crystallite size is higher than the micropore size [26].

On the other hand, carbonaceous support had no significant influence on the crystallite size growing. It is stated regarding that the Pt crystallite sizes for the untreated Vulcan and a-BC had very similar values, with the exception of the physically activated Vulcan. Something similar took place in the case of the PtSn alloy that for all the supports indistinctly had very similar crystallite size values.

Cyclic voltammetry

Electrocatalysts systems (Table 2) electrochemical behavior was evaluated by cyclic voltammetry in 1.0 M ethanol and 0.5 M H_2SO_4 solution.

Voltammograms reveal the electrochemical behavior for platinum-based alloys in acidic medium, with two oxidation peaks, one in direct scan, and the other in reverse scan. This voltammetric profile has been reported elsewhere [14,20,24]. The peak in direct sweep can be related to oxidation reactions of alcohol, whereas the one in reverse sweep could be associated to incompletely oxidized carbonaceous residues on the catalyst surface [24].

The maximum current density values (i) developed by the analyzed catalyst and their respective potential (E_{max}) were determined from Fig. 3. E_{max} corresponds to the potential at which the highest current density is developed. The smaller E_{max} values, the better the supported catalyst performance. These data allow obtaining information about catalytic activity of synthesized catalysts. Another important parameter in this evaluation is the onset potential (E_{onset}), which corresponds to the potential where currents start to increase. All of these data are shown in Table 6.

Both Vulcan and a-Vulcan supported Pt and PtSn showed similar ethanol oxidation potentials, i.e., in the direct scan; related to those systems, this potential is lower for biocarbon supported platinum and higher for biocarbon supported PtSn.

Commercial carbon Vulcan supported platinum showed the highest current densities, compared to the biocarbon supported platinum. May be, it can be related to the sulfur content, regarding that, as some authors [27] report, sulfur has a significant affinity with platinum, makes the catalyst more stable and improves its catalytic activity.

Supported PtSn alloys developed higher current density than Pt, revealing a better performance for the catalysts with Sn addition for ethanol electro-oxidation; i.e. Sn enhances the catalyst activity (Fig. 3b and Table 6). Also, the presence of Sn improves the catalytic activity that can be related to the effect of lattice contraction and the small crystallite size [28]. The modified electronic structure of platinum weakens the CO adsorption, which reduces the catalyst poisoning [29–32]. Biocarbon supported PtSn electrocatalyst had the highest current density in the direct (anodic) scan, compared to the both commercial Vulcan carbons, in as far as it showed a decrease in the ethanol oxidation startup potential (Table 6). It proves the viability of biocarbon for applications in fuel cells.

An important parameter in cyclic voltammetry analysis is the standard deviation in the current density and potential values. Standard deviation can be associated to the heterogeneity in the electrocatalyst structure [14]. A high potential deviation could indicate the presence of different metallic phases, as a high current density deviation can be related to a heterogeneity toward metal particle distribution on the carbon surface. In the synthesized electrocatalysts, it is not possible to verify a significant variation in the potential values (Table 6), indicating the presence of few phases, or just one, which is in agreement with the deposition of only one metal and the alloy formation for the Pt and Sn deposition. The standard deviation of current densities values observed is probably associated to the irregularity in the distribution of the particles on the carbon surface [14]; since standard deviation of current density are, in general, very low, particle distribution seems to be homogeneous throughout the carbon surface, especially for the biocarbon.

Pt and PtSn deposition on carbonaceous supports is enhanced by the carbon surface chemistry since oxygenated

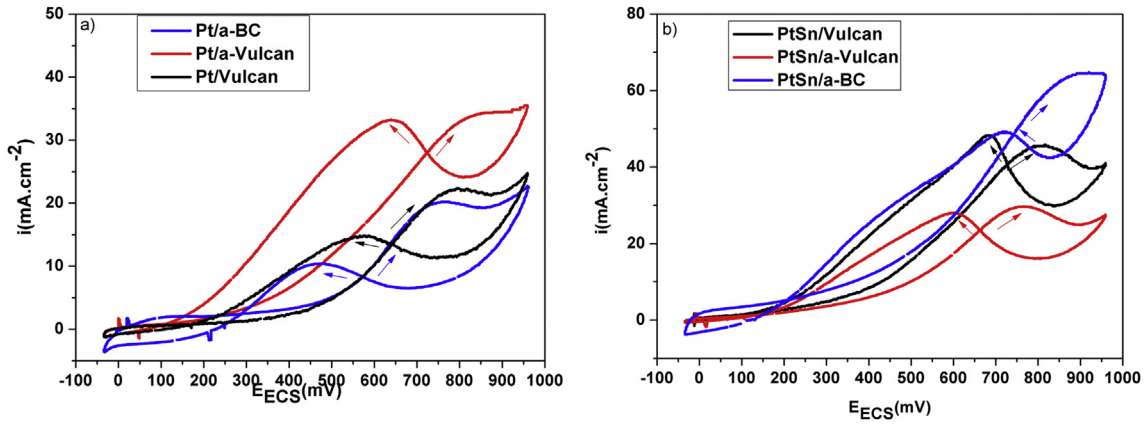

Fig. 3 – Cyclic voltammogram for the Vulcan, a-Vulcan and a-BC supported a) Pt and b) PtSn.

Please cite this article in press as: da Silva EL, et al., Influence of activated carbon porous texture on catalyst activity for ethanol electro-oxidation, International Journal of Hydrogen Energy (2014), http://dx.doi.org/10.1016/j.ijhydene.2014.07.103

functional groups constitute preferential sites for the development of the ligand chemistry that allows the metal reduction and, hence, the metal deposition [29,30]. Due to the low values of the standard deviation in the electrochemical results it is possible to propose that there was a uniform deposition of the platinum on the Vulcan and a-Vulcan carbons and of the alloy PtSn on biocarbon. These characters can be explained by the surface chemistry of the carbons, since the presence of oxygenated groups (phenolic, lactonic and carboxylic) seem to be preferential sites for the platinum and alloy depositions, regarding the FTIR spectra and the elemental analysis. However, the preferential groups for the metal and the alloy depositions need further study to be determined [30].

Onset potentials reveal that the oxidation of the species starts at lower potentials for untreated Vulcan and a-BC carbons supported PtSn alloy. It involves less external power supply in order to startup the electrochemical reactions, as well as in the DEFC operation [14]. Since untreated Vulcan and a-BC carbons supported PtSn crystallite sizes are 3.03 and 3.15 nm, perhaps the catalyst has a suitable nanoparticle distribution throughout the whole catalyst support surface area that enhances the profiting of the catalytic surface area, hence, the catalyst activity, and ensures the electrolyte accessibility to the active sites due to the better catalyst dispersion on the support. Regarding pure platinum catalyst, a-Vulcan support with 3.0 nm crystallite size is suitable to reduce the onset potentials that have values of 100 mV higher in comparison with the other two carbon supports Vulcan and a-BC.

Untreated Vulcan and a-Vulcan supported Pt and PtSn catalysts performance did not show a significant support influence on the potentials and current densities during the anodic and cathodic scan. It was concluded by the voltammetry values in Table 6, that they are very similar to each other. However, their onset potentials differ depending on the cristallyte size of the catalyst, as it was aforementioned.

Conclusion

Activated carbons obtained by physical activation of eucalyptus wood and a commercial Vulcan XC72R were tested as Pt and PtSn catalyst support, for application in DEFC. For platinum catalyst, the commercial carbon supports showed good performances regarding that platinum deposited on them has the smallest crystallite size. PtSn was very well dispersed on biocarbon, with small particle size, and has good electrochemical performance on this support. Biocarbon showed a higher surface area than the commercial activated carbons. X-Ray diffraction confirmed the Pt deposition on the catalyst supports and it was demonstrated that Pt and Sn deposition involves an alloy formation. The best electrochemical performance corresponded to biocarbon supported PtSn alloy, since its current densities and peak potentials were the highest and it onset potentials, the lowest. According to this, it can be stated that biocarbon are adequate for fuel cell applications. Also, since electrochemical behaviors differ among supports, it can be concluded that support influenced in the different catalyst performance.

Acknowledgments

Authors would like to thank the financial support of the Brazilian agencies Coordination for the Improvement of Higher Education Personnel – CAPES, National Council for Scientific and Technological Development – CNPq and Research Support Foundation in Rio Grande do Sul State – FAPERGS.

REFERENCES

[1] Assumpção MHMT, Nandenha J, Buzzo GS, Silva JCM, Spinacé EV, Neto AO, et al. The effect of ethanol concentration on the direct ethanol fuel cell performance and products distribution: a study using a single fuel cell/attenuated total reflectance – fourier transform infrared spectroscopy. J Power Sources 2014;253:392–6.
[2] Iwasita T, Pastor E. A dems and FTir spectroscopic investigation of adsorbed ethanol on polycrystalline platinum. Electrochim Acta 1994;39:531–7.
[3] Gonzalez Ernesto R. Eletrocatálise e poluição ambiental. Quím Nova 2000;23:262–6.
[4] Antolini E. Catalysts for direct ethanol fuel cells. J Power Sources 2007;170:1–12.
[5] Van der Lee MK, van Dillen J, Bitter JH, de Jong KP. Deposition precipitation for the preparation of carbon nanofiber supported nickel catalysts. J Am Chem Soc 2005;127:13573–82.
[6] Gangeri M, Perathoner S, Centi G. Synthesis and performances of carbon-supported noble metal nanoclusters as electrodes for polymer electrolyte membrane fuel cells. Inorg Chim Acta 2006;359:4828–32.
[7] Rajesh B, Karthik V, Karthikeyan S, Ravindranathan Thampi K, Bonard J-M, Viswanathan B. Pt–WO3 supported on carbon nanotubes as possible anodes for direct methanol fuel cells. Fuel 2002;81:2177–90.
[8] Toebes ML, van der Lee MK, Tang LM, Huis in 't Veld MH, Bitter JH, van Dillen AJ, et al. Preparation of carbon nanofiber supported platinum and ruthenium catalysts: comparison of Ion adsorption and homogeneous deposition precipitation. J Phys Chem B 2004;108:11611–9.
[9] Liu H, Song C, Zhang L, Zhang J, Wang H, Wilkinson DP. A review of anode catalysis in the direct methanol fuel cell. J Power Sources 2006;155:95–110.
[10] Bansal RC, Donnet JB, Stoeckli F. Active carbons. New York: M. Dekker; 1988.
[11] Savova D, Apak E, Ekinci E, Yardim F, Petrov N, Budinova T, et al. Biomass conversion to carbon adsorbents and gas. Biomass Bioenergy 2001;21:133–42.
[12] Suárez AC, Tancredi N, Pinheiro PCC, Yoshida MI. Thermal analysis of the combustion of charcoals from Eucalyptus dunnii obtained at different pyrolysis temperatures. J Therm Anal Calorim 2010;100:1051–4.
[13] Amaya A, Medero N, Tancredi N, Silva H, Deiana C. Activated carbon briquettes from biomass materials. Bioresour Technol 2007;98:1635–41.
[14] S. Correa P dos, da Silva EL, da Silva RF, Radtke C, Moreno B, Chinarro E, et al. Effect of decreasing platinum amount in Pt–Sn–Ni alloys supported on carbon as electrocatalysts for ethanol electrooxidation. Int J Hydrogen Energy 2012;37:9314–23.
[15] D28 Committee. Test method for total ash content of activated carbon. ASTM Int 2011. Book of Standards 15.01.

Please cite this article in press as: da Silva EL, et al., Influence of activated carbon porous texture on catalyst activity for ethanol electro-oxidation, International Journal of Hydrogen Energy (2014), http://dx.doi.org/10.1016/j.ijhydene.2014.07.103

[16] Jiang L, Sun G, Zhou Z, Zhou W, Xin Q. Preparation and characterization of PtSn/C anode electrocatalysts for direct ethanol fuel cell. Catal Today 2004;93–95:665–70.
[17] Linares-Solano A, Lozano-Castelló D, Lillo-Ródenas MA, Cazorla- Amorós D. Carbon activation by alkaline hydroxides – preparation and reactions, porosity and performance. Chem. Phys. Carbons, vol. 30. Boca Raton, FL: CRC Press Taylor & Francis Group, LLC; 2010. p. 1–62.
[18] Lillo-Ródenas MA, Cazorla-Amorós D, Linares-Solano A. Understanding chemical reactions between carbons and NaOH and KOH: an insight into the chemical activation mechanism. Carbon 2003;41:267–75.
[19] Stuart B. Infrared spectroscopy: fundamentals and applications. Chichester, West Sussex: John Wiley & Sons Ltd; 2004.
[20] Zhou W, Zhou Z, Song S, Li W, Sun G, Tsiakaras P, et al. Pt based anode catalysts for direct ethanol fuel cells. Appl Catal B Environ 2003;46:273–85.
[21] Chatterjee M, Chatterjee A, Ghosh S, Basumallick I. Electro-oxidation of ethanol and ethylene glycol on carbon-supported nano-Pt and -PtRu catalyst in acid solution. Electrochim Acta 2009;54:7299–304.
[22] Kittel. Introduction to solid state physics. 5th ed. New York: John Wiley & Sons, Inc.; 1976.
[23] Callister. Ciência e Engenharia de Materiais: Uma Introdução. Quinta edição. Rio de Janeiro: LTC; 2002.
[24] Kim JH, Choi SM, Nam SH, Seo MH, Choi SH, Kim WB. Influence of Sn content on PtSn/C catalysts for electrooxidation of C1–C3 alcohols: synthesis, characterization, and electrocatalytic activity. Appl Catal B Environ 2008;82:89–102.
[25] Colmati F, Antolini E, Gonzalez ER. Ethanol oxidation on a carbon-supported Pt75Sn25 electrocatalyst prepared by reduction with formic acid: effect of thermal treatment. Appl Catal B Environ 2007;73:106–15.
[26] Rodríguez-Reinoso F, Molina-Sabio M. Activated carbons from lignocellulosic materials by chemical and/or physical activation: an overview. Carbon 1992;30:1111–8.
[27] Kiciński W, Szala M, Bystrzejewski M. Sulfur-doped porous carbons: synthesis and applications. Carbon 2014;68:1–32.
[28] Isaifan RJ, Ntais S, Baranova EA. Particle size effect on catalytic activity of carbon-supported Pt nanoparticles for complete ethylene oxidation. Appl Catal Gen 2013;464–465:87–94.
[29] Calvillo L, Gangeri M, Perathoner S, Centi G, Moliner R, Lázaro MJ. Effect of the support properties on the preparation and performance of platinum catalysts supported on carbon nanofibers. J Power Sources 2009;192:144–50.
[30] Chen S, Xu R, Huang H, Yi F, Zhou X, Zeng H. Reduction–adsorption behavior of platinum ions on activated carbon fibers. J Mater Sci 2007;42:9572–81.
[31] Zhu M, Sun G, LI H, Cao L, Xin Q. Effect of the Sn (II)/Sn (IV) redox couple on the activity of PtSn/C for ethanol electro-oxidation. Chin J Catal 2008;29:765–70.
[32] Tayal J, Rawat B, Basu S. Bi-metallic and tri-metallic Pt–Sn/C, Pt–Ir/C, Pt–Ir–Sn/C catalysts for electro-oxidation of ethanol in direct ethanol fuel cell. Int J Hydrogen Energy 2011;36:14884–97.

Please cite this article in press as: da Silva EL, et al., Influence of activated carbon porous texture on catalyst activity for ethanol electro-oxidation, International Journal of Hydrogen Energy (2014), http://dx.doi.org/10.1016/j.ijhydene.2014.07.103